INVESTIGATING THE NONLINEAR DYNAMICS OF NATURAL-CIRCULATION, BOILING TWO-PHASE FLOWS

THERMAL HYDRAULICS

KEYWORDS: *boiling two-phase flow, nonlinear dynamics, chaotic oscillations*

ROBERT ZBORAY* and WILHELMUS J. M. DE KRUIJF
Delft University of Technology, Interfaculty Reactor Institute, The Netherlands

TIM H. J. J. VAN DER HAGEN *Delft University of Technology*
Interfaculty Reactor Institute and Kramers Laboratorium voor Fysische Technologie
The Netherlands

RIZWAN-UDDIN *University of Illinois*
Department of Nuclear, Plasma, and Radiological Engineering
103 S. Goodwin Avenue, Urbana, Illinois 61801

Received March 3, 2003
Accepted for Publication January 12, 2004

The nonlinear dynamics of natural-circulation, boiling two-phase flows are investigated using a two-phase flow loop. Experiments have been carried out in the unstable operating region of the facility for various system pressures and for different frictions at the exit of the riser section. It appears that the boiling two-phase flow undergoes the well-known Feigenbaum scenario, the period-doubling route toward chaotic behavior. Evaluation of the recorded signals using nonlinear time series analysis methods indicates the occurrence of chaotic density-wave oscillations.

I. INTRODUCTION

Natural-circulation, boiling two-phase flows are widely applied in industrial systems like heat exchangers and boilers. The application of natural circulation of the coolant in boiling water nuclear reactors (BWRs) has gained interest in the last decades because it results in more economical and safer designs than present-day, forced-circulation BWRs.

A major concern for the safe operation of the aforementioned industrial boiling, two-phase flow systems is to avoid the occurrence of so-called density-wave oscillations. Density-wave oscillations in heated channels have been studied for a long time, and the progress in this field has continuously been reviewed.[1–3] Thanks to the considerable research effort, significant success has been achieved in explaining and identifying the main physical mechanisms involved in density-wave oscillations.

The mechanism of density-wave oscillations in boiling channels can be explained in a number of equivalent ways. The most commonly accepted explanation is as follows: Channel inlet flow perturbations create enthalpy fluctuations in the single-phase region. At the boiling boundary (the elevation at which the bulk of the liquid reaches the saturation temperature and starts to boil), the enthalpy perturbations are transformed into void-fraction variations that travel with the flow through the system. Obviously, the position of the boiling boundary fluctuates as well. The combined effect of flow, void-fraction, and boiling-boundary perturbations causes fluctuations in the pressure drop across the channel. Since the total pressure drop across the channel is imposed externally by the characteristics of the system feeding the channel, variations in the pressure drop produce a feedback perturbation in the inlet flow. Under specific conditions, the pressure-drop perturbations can acquire appropriate phases, and the inlet flow oscillations become self-sustained. It is clear that transportation-delay and pressure-drop characteristics are of paramount importance for the stability of the system.

Although the current understanding of density-wave oscillations is fairly good for *linear* phenomena,[4] more work is needed to understand *nonlinear* dynamics and *unstable* behavior. For validating codes for these operational regimes, the experimental database on the dynamics of natural circulation should be broadened. There is

*E-mail: robert.zboray@psi.ch

no confidence that state-of-the-art codes are able to reproduce within acceptable margins the behavior of natural-circulation, boiling two-phase flows, particularly in regimes of highly nonlinear, unstable behavior, where modeling assumptions might play a more pronounced role than in the more conventional, linear regime.

Several attempts to model the nonlinear dynamics of boiling flows can be found in the literature. Achard et al.[5] have performed analytical Hopf-bifurcation analysis of a boiling channel using the homogeneous-equilibrium model. It was later extended by Rizwan-uddin and Dorning[6] using the drift-flux model and nonuniform heater profiles. As another approach, fully numerical studies have been carried out as well. Rizwan-uddin and Dorning[7,8] have shown that two-phase flow in a vertical heated channel subjected to periodical forcing exhibits a strange attractor. Clausse and Lahey[9] developed a model based on the homogeneous-equilibrium approach and found limit-cycle oscillations and a strange attractor for a single channel with uniform heat flux. Extending that model, Chang and Lahey[10] predicted a period-doubling sequence and chaotic oscillations for a heated channel coupled with an adiabatic riser.

As for the *experimental* investigation of the nonlinear dynamics of boiling flows, the experiments are usually restricted to the determination of the threshold of instability and to parametric studies on that, e.g., Saha et al.,[11] Furutera,[12] Delmastro et al.,[13] and Kyung and Lee[14,15] have performed an extensive measurement campaign on the stability of a natural-circulation Freon loop. They encountered a region of excursive instability inside the unstable region, at very high subcooling, which could result in "periodic flow excursions." However, to the authors' knowledge, no experimental findings have ever been reported about chaotic dynamics or period-doubling sequences in boiling systems.

In the present paper, investigations on the nonlinear dynamics of natural-circulation, boiling two-phase flows are discussed concerning density-wave instabilities. Experiments have been carried out using the Delft Simulated Reactor (DESIRE) facility, a natural-circulation loop. The facility is described briefly in Sec. II. Thereafter, measurements on the nonlinear dynamics of the system are presented. Measured time traces are analyzed using nonlinear time series methods.

II. THE EXPERIMENTAL FACILITY

II.A. Dimensions and Instrumentation

The DESIRE facility is a natural-circulation, boiling two-phase flow loop using Freon-12 as a working fluid.[16] The central part of the facility consists of a 6×6 array of electrically heated rods, which is a scaled copy of one fuel assembly of a BWR. A tall riser section is placed on top of the heated assembly ("core") to enhance the natural-circulation flow rate, which is maintained by the density difference between the vapor-liquid mixture in the assembly+riser and the liquid in the downcomer section. The scheme of the loop is shown in Fig. 1. Two sets of electrical heater rods can be used in the facility: one set with a uniform axial power profile, the other with a sinus+offset profile. For the latter, the pitch of the coils of the resistance wire is a function of the position in the rod in such a way that the axial power profile is

$$P'(z) = P \frac{\left(1 - \frac{2}{\pi} f_p\right) + (f_p - 1)\sin\left(z \frac{\pi}{L}\right)}{L\left(1 - \frac{2}{\pi}\right)} , \quad (1)$$

where

P = total power

z = axial elevation

L = length of the rods

f_p = axial power peaking factor, which has a value of 1.4.

A flow-resistance element with variable friction is installed on top of the riser section. This enables the study of density-wave oscillations in DESIRE since a high outlet (two-phase) friction tends to destabilize the two-phase flow (see below).

The facility is fully equipped with pressure, temperature, and flow sensors. A gamma-transmission setup with an ^{241}Am source is used to measure the area-averaged void fraction at different heights along the assembly in broad gamma beam geometry. The diameter of the gamma beam is ~2 cm, whereas the width of the assembly is 5.4 cm.

II.B. System Behavior in the Stable Operating Region

To quantify the linear stability of the system, the so-called decay ratio (DR) is used. The DR is defined as the ratio between two consecutive maxima of the impulse response function of the system. The DR is smaller than unity for a stable system (with a damped response), and it is equal to or larger than unity for an oscillatory, unstable system. If the system is driven by wideband (white) noise, the DR can also be extracted from the consecutive maxima of the autocorrelation function (ACF) of measured dynamical variables of the system. The ACF of signal $x(t)$ is defined as[17]

$$\mathrm{ACF}(\tau)_{x(t)} \equiv \lim_{T\to\infty} \frac{\frac{1}{T}\int_0^T x(t)x(t+\tau)\,dt}{\frac{1}{T}\int_0^T x(t)^2\,dt} . \quad (2)$$

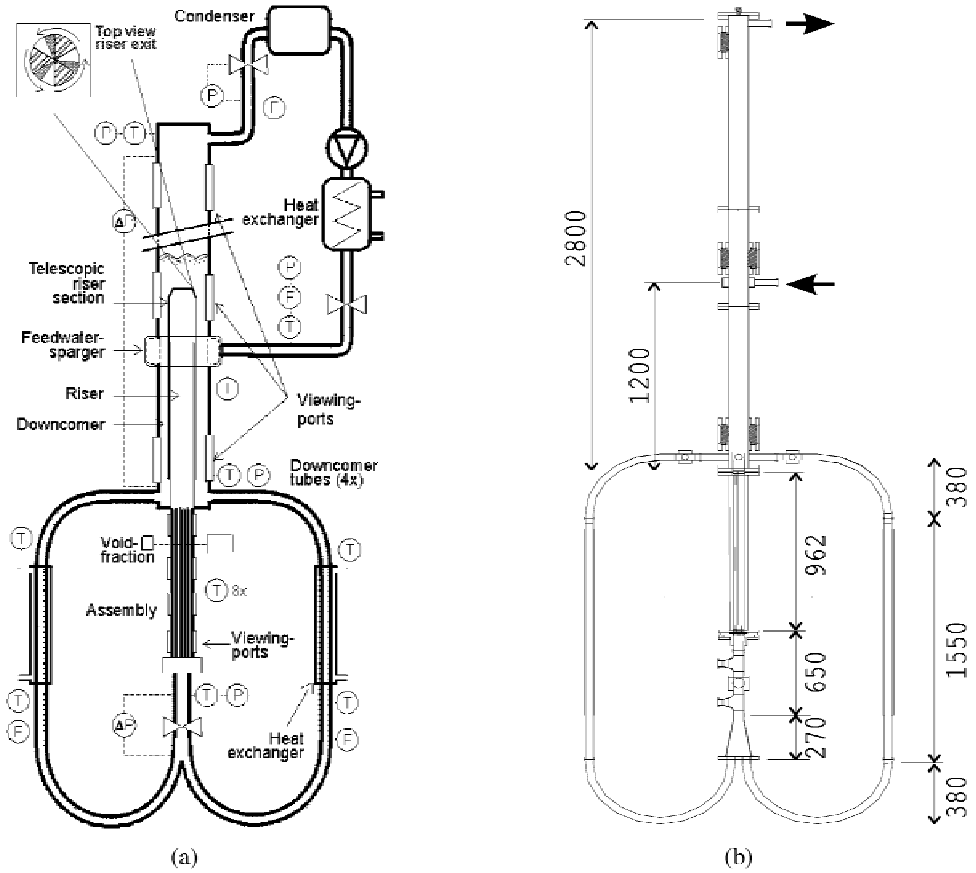

Fig. 1. Scheme of the DESIRE facility. (a) *P*, *T*, and *F* denote pressure, temperature, and flow sensors, respectively. (b) The dimensions of the facility are shown. The length of the heated section is 962 mm; the liquid flows upward in this section; the length of the riser section is 1400 mm.

The ACF of the inlet mass-flow rate and void-fraction signals are used here to obtain the DR.

Experimental series have been carried out to examine the linear stability of the DESIRE facility at different settings of the riser-exit friction element.[18] All of these measurements have been performed at a nominal system pressure of 11.6 bars.

As an example, measurement points for a series performed for a uniform axial power profile are given in terms of the dimensionless Zuber (or phase-change) number (N_{Zu}) and the subcooling number (N_{sub}) in Fig. 2. These two dimensionless numbers are commonly used in the analysis of boiling, two-phase flow systems. The former one is proportional to the total power to inlet mass-flow ratio, and the latter one is proportional to the inlet subcooling:

$$N_{Zu} \equiv \frac{P}{\phi(h_g - h_l)} \frac{\rho_l - \rho_g}{\rho_g}$$

and

$$N_{sub} \equiv \frac{h_l - h_{in}}{h_g - h_l} \frac{\rho_l - \rho_g}{\rho_g} \quad , \tag{3}$$

where

P = total assembly power

ϕ = inlet mass-flow rate

h_l, ρ_l = saturated liquid enthalpy and density, respectively

h_g, ρ_g = vapor enthalpy and density, respectively

h_{in} = specific liquid enthalpy at the assembly inlet.

It can be seen from the DR values in Fig. 2a that moving toward higher N_{Zu} and N_{sub}, the DR, in general, is increasing; i.e., the two-phase flow becomes gradually less stable. For indicative purposes only, several equi-DR lines are drawn in Fig. 2a obtained by interpolating on the measurement points. Figure 2b compares the stability for two riser-exit friction settings. It shows that the DR is larger at about the same operating point for a higher riser-exit friction. This destabilizing effect of an increased two-phase (exit) friction on density-wave oscillations is well known from literature on two-phase flow dynamics.[1,11]

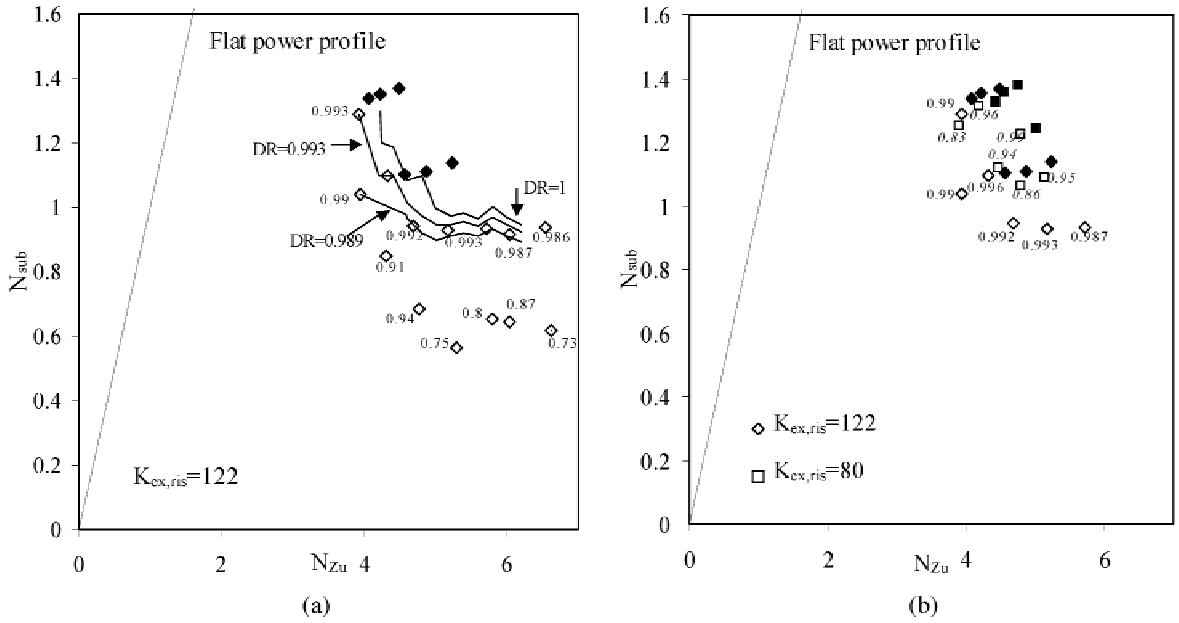

Fig. 2. The stability behavior of the system showing measurement points in the N_{Zu}-N_{sub} plane for uniform power profile settings. The numerals are the measured DRs indicated near the points. Solid symbols indicate unstable points (limit-cycle oscillations, DR = 1); open symbols indicate stable operating points. (a) Results obtained for riser-exit friction factor $K_{ex,ris}$ = 122. Several equi-DR lines are drawn in this figure (obtained by cubic interpolation of the measured values) for indicative purposes. (b) Comparison of the stability for two riser-exit friction settings; the uncertainty of the DR values is ~1 to 2%; the uncertainty of the operating points (N_{Zu}-N_{sub}) is ~4 to 5%.

Several operating points of Fig. 2 are indicated to be unstable (DR = 1). In these points, which lie in the unstable operating region of the facility, constant-amplitude oscillations are measured. These, so-called, limit-cycle oscillations are typical nonlinear phenomena for which the initially small-amplitude, growing oscillations are bounded by nonlinear effects when the oscillation amplitude becomes large.

The behavior of the natural-circulation two-phase flow in operating points deep in the unstable operating region is described in Sec. III.

III. INVESTIGATING THE NONLINEAR DYNAMICS

III.A. Experimental Results

The experiments in the unstable operating region have been carried out for different system pressures and for various distributions of the frictional pressure drops in the single- and two-phase regions. The latter is achieved by varying the friction coefficient of the adjustable flow resistance element at the riser exit. A sinus+offset heating-power profile has been used in all the measurements. The influence of the axial-power profile on the nonlinear dynamics of natural-circulation two-phase flows has been investigated in Zboray et al.,[19] and it is not examined further here.

The following procedure has been followed in all cases: Starting from a stable operating condition, the heating power is gradually increased, in steps, while keeping all other controllable system parameters constant and waiting at each step until transients die out and the system reaches asymptotic behavior. The following scenario has been observed in all cases with different system pressures and with various frictions at the riser exit: As the power reaches the threshold of stability, the fixed point becomes unstable; it undergoes a supercritical Hopf bifurcation,[20] and limit-cycle flow oscillations result. As the power reaches another critical value, the system undergoes a next bifurcation: a so-called period-doubling bifurcation. At this point, oscillations with two different amplitudes and with a period twice the period of the original oscillations arise. The occurrence of two such consecutive bifurcations indicates the onset of the well-known Feigenbaum scenario.[21]

In the Feigenbaum scenario, a cascade of successive period-doubling bifurcations takes place as a system parameter (the so-called bifurcation parameter) is being varied in a nonlinear system, and the aperiodic (chaotic) behavior starts off as the bifurcation parameter is varied beyond a critical value. After each period doubling, the number of different oscillation amplitudes is doubled,

which corresponds to the appearance of successive subharmonic components in the frequency spectrum of the oscillations. According to Feigenbaum's theory,[21] this scenario possesses certain universal features; namely, the critical values of the successive period-doubling bifurcations converge in an asymptotically geometric manner toward the aperiodic limit. The convergence ratio is a universal number, the Feigenbaum-delta ($\delta = 4.6692\ldots$). Another universal scaling feature of the scenario is that the ratio of the amplitudes of the consecutive subharmonic components in the spectrum converges to: $\mu = 6.5573\ldots$.

Representative oscillation patterns and the corresponding Fourier spectra for the aforementioned behavior of the two-phase flow in the DESIRE facility are shown in Fig. 3. The maxima and minima of the oscillations are shown in Fig. 4 as a function of the power. Running at 25.5 kW, the mass-flow rate shows a constant-amplitude, limit-cycle oscillation (Fig. 3a). The spectrum indicates that the oscillation is not sinusoidal at all but contains many higher harmonics. The maximum and the minimum of this oscillation correspond with the two symbols at 25.5 kW in Fig. 4. Figure 4 shows that the flow starts to oscillate at a power of ~18 kW, with increasing amplitude as the power is increased. Increasing the power from 25.5 to 28.4 kW leads to the first period doubling: The flow oscillates now with a high and a low maximum and a high and a low minimum. Consequently, Fig. 4 shows the four corresponding symbols at 28.4 kW. A peak appears in the spectrum at half the original resonance frequency (a subharmonic); its harmonics show up as well. Increasing the power just a bit more to 32.3 kW leads to chaotic behavior (Fig. 3c); correspondingly, the number of maxima and minima becomes infinite, some of which are indicated by small dots in Fig. 4. The spectrum does not contain clear resonance peaks any longer. The measured transition from limit-cycle oscillations to chaotic oscillations is illustrated also in the bifurcation diagram in Fig. 5.

The finer details of the Feigenbaum scenario—the cascade of period-doubling bifurcations—could not be detected conclusively. Because of the relatively large value of δ, the consecutive bifurcation points—after the first few period doublings—cannot be distinguished from each other in terms of the bifurcation parameter due to the finite resolution of the measurement. Because of the scaling with μ, the amplitude of the successive subharmonics (i.e., the vertical spacing of symbols in Fig. 4) becomes very small for practical (measurement) purposes after a few period doublings as well. Obviously, the presence of measurement noise diminishes further the possibility to identify subsequent bifurcations. The small spectral peaks corresponding to higher-order bifurcations disappear in the noisy background spectrum (e.g., due to the boiling noise). Nevertheless, in all cases, a gradual and clear change can be observed in the measured oscillation patterns and in the corresponding spectra (a gradual broadening of the peaks and a peculiar increase in the broadband background; see Fig. 3c) as the power is increased past the first period-doubling bifurcation point.

Since the discovery of the universality features of the period-doubling route toward chaotic behavior, this scenario has been observed experimentally in a broad variety of small-scale physical systems including nonlinear electronic circuits,[22] Rayleigh-Bènard cells,[23] optically bistable laser cavities,[24] and superfluid helium.[25] However, in large-scale physical, mechanical systems prone to high noise levels, even the onset of the scenario (the first period doubling) has not been reported. For example, although predicted with theoretical models by Clausse and Lahey[9] and by Chang and Lahey,[10] it has not been observed yet in boiling two-phase flow systems. To the authors' knowledge, the results presented here are the first experimental evidence suggesting that a large, boiling two-phase flow system undergoes the Feigenbaum scenario.

The influence of system pressure on the bifurcation sequence is studied by repeating the experiments for two different values of system pressure and the same riser exit friction factor. Table I summarizes the experimental findings for four experimental cases. The power at which the system starts to oscillate (P_0), the power of the first bifurcation (P_1), and the measured chaotic limit (P_∞) are given. Using the Feigenbaum-delta, the chaotic limit is also estimated from the previous critical power values assuming geometric convergence with δ as

$$P_\infty^{est} = P_1 + \frac{P_1 - P_0}{\delta} \quad . \tag{4}$$

The estimated values of the chaotic limit are somewhat lower than the actually observed chaotic limit. The discrepancy is believed to be due to the fact that in reality the convergence is asymptotically geometric.

Period doubling in experiment series 3 could not be clearly detected, and hence, the effect of system pressure on the bifurcation sequence is not clear. The effect of changing the pressure drop in the two-phase region was studied by varying the riser-exit friction factor (series 1 and 4). Decreasing the frictional pressure drop at the riser exit tends to increase the critical bifurcation values and the chaotic power limit (P_∞); it also tends to stretch the interval between the Hopf bifurcation and the period-doubling bifurcation. Similar observations can be made comparing series 1 to series 3 (although for the latter the period-doubling bifurcation point is not clear).

It is not very instructive to try to extract features of a nonlinear system by just looking at the power spectrum. To qualify and quantify the system behavior in the presumed chaotic region, methods developed for nonlinear and chaotic time series analysis are of use. These methods are described and applied in Sec. III.B.

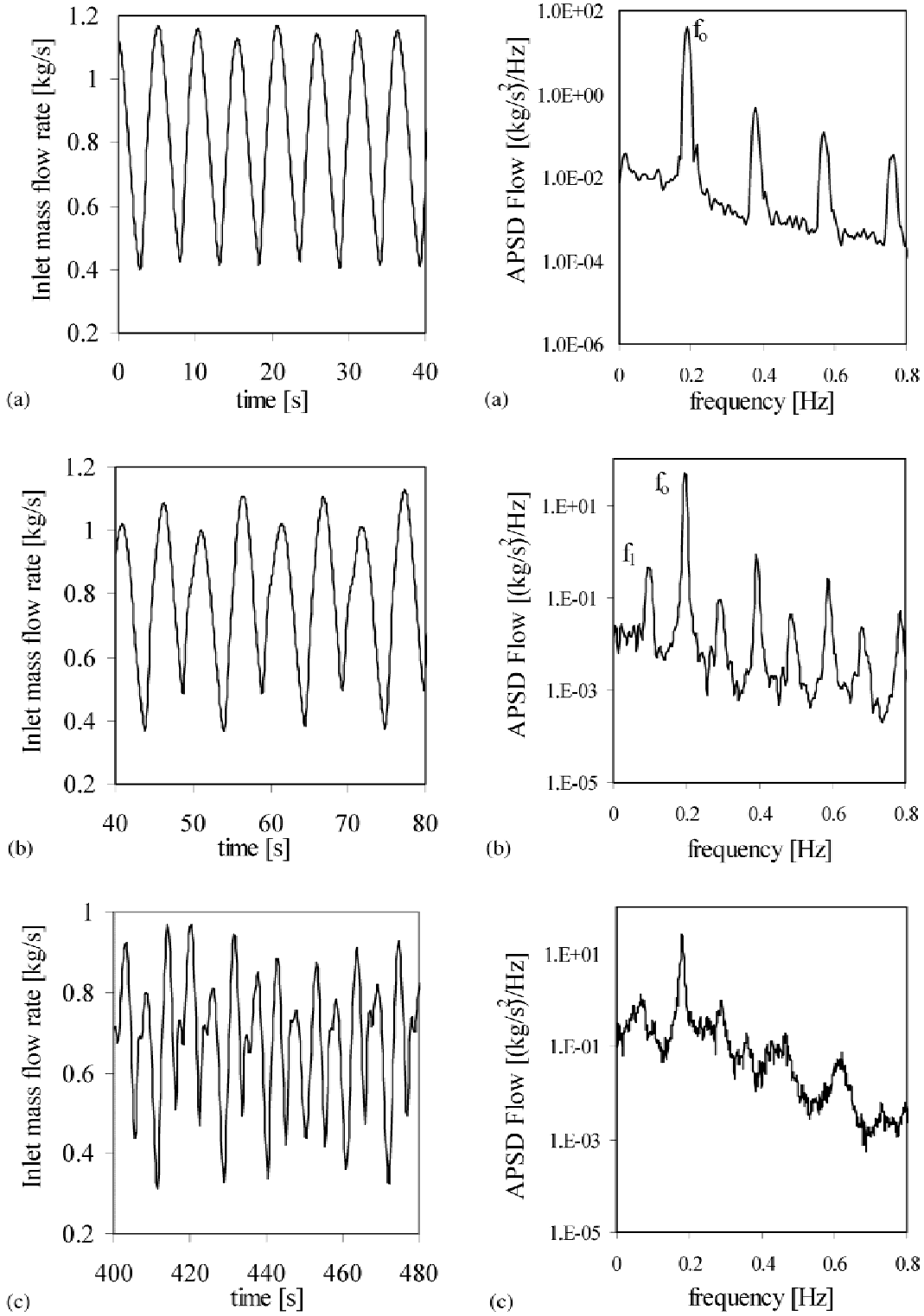

Fig. 3. Inlet flow rate oscillation patterns and the corresponding autopower spectral density (APSD) for a system pressure of 11.6 bars and a friction factor at the riser exit of 118 ± 18. (a) Beyond the threshold of stability (at 25.5 kW power), the appearance of numerous higher harmonic components in the APSD indicates the strongly nonlinear character of the oscillations. (b) Just beyond the first period-doubling point (at 28.4 kW power), the oscillation period is twice of that at 25.5 kW. Correspondingly, a halved frequency component (f_1, the first subharmonic) appears in the spectrum next to f_0. (c) Further beyond the first period-doubling bifurcation (at 32.3 kW power), the oscillations are chaotic. (The figures are based on series 1 from Table I.)

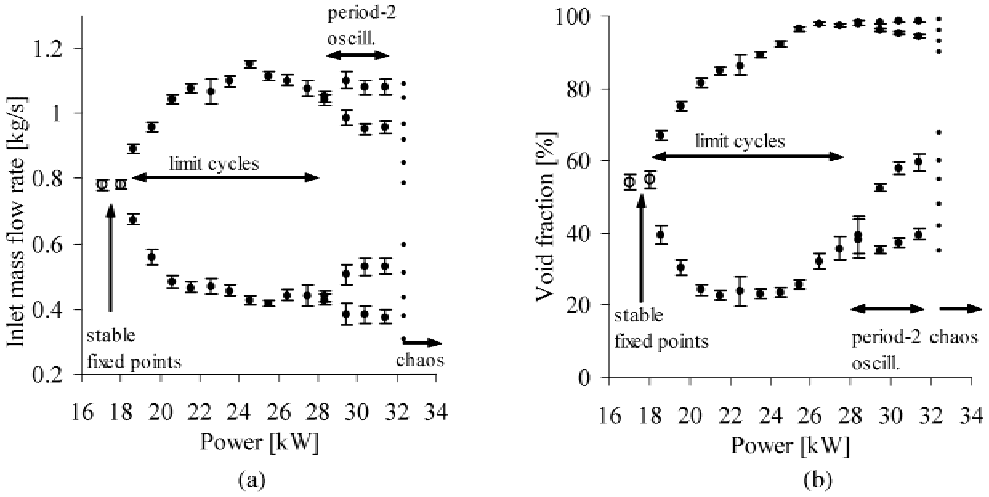

Fig. 4. The plots show the minima and maxima of the flow-rate and void-fraction oscillations as a function of power measured at a system pressure 11.6 bars and with a riser-exit friction factor of 118 ± 18. The hollow dots show two stable fixed points at low power just under the Hopf-bifurcation point. Several measured oscillation minima and maxima depicted at 32.3 kW illustrate chaotic oscillations. The arrows indicate the regimes of different oscillation modes

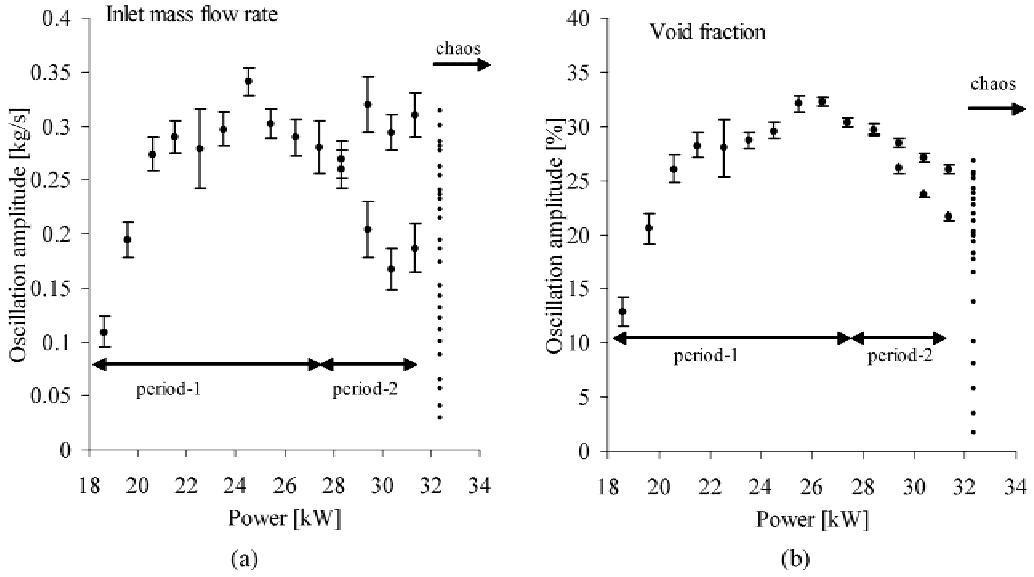

Fig. 5. Bifurcation diagram showing the oscillation amplitudes as a function of the power for the different measured oscillation modes. The small dots show measured chaotic oscillation amplitudes at 32.3 kW.

III.B. Nonlinear Time Series Analysis

A vast literature exists on methods to detect and quantify chaos in measured time series.[26,27] Three chaos descriptors are determined here for the measured signals: the Kolmogorov entropy, the correlation dimension, and the maximum Lyapunov exponent. The algorithms for determining these quantities are based on the reconstruction of the chaotic (strange) attractor in the state-space of the system using the time-delay embedding technique.[28] Given the measured time series $x(i)$ with $i = 1, \ldots, N$ and sampling time τ, the reconstruction vectors of dimension d are formed as

$$X(i) = (x(i), x(i+T), \ldots, x(i+(d-1)T)) \ , \quad (5)$$

where T and d are the time delay and the embedding dimension, respectively. The embedding dimension that

TABLE I

Measured Critical Values of Heating Power for the Transition to Oscillatory Behavior P_0, for the First Period-Doubling Bifurcation P_1, and for the Chaotic Oscillations P_∞*

Series	Pressure (bar)	$K_{ex,ris}$	P_0 (kW)	P_1 (kW)	P_∞ (kW)	P_∞^{est} (kW)
1	11.6	118 ± 18	18.0 ± 0.3	27.4 ± 1.0	32.3	30.0 ± 1.3
2	8.4	145 ± 17	15.2 ± 0.3	24.6 ± 1.0	29.3	27.1 ± 1.4
3	11.2	145 ± 17	16.2 ± 0.5	—	31.3	—
4	12.2	110 ± 7	24.0 ± 0.4	38.2 ± 1.0	45.9	42.1 ± 1.4

*Also shown are the estimated threshold values for transition to chaos P_∞^{est}. Experimental conditions (pressure, riser-exit friction factor, and $K_{ex,ris}$) are given as well.

we use in the following analyses is typically ~50 with $T = 1$.

III.B.1. The Kolmogorov Entropy

The Kolmogorov entropy K characterizes the *dynamics* (time evolution) of chaotic behavior. One divides the state-space into small cells and follows the time evolution of the system using a collection of initial conditions located all within one cell. After N time steps of length τ, when the trajectories generally are already spread out over a large number of cells, the entropy S_N is calculated using

$$S_N = -\sum_r p_r \ln p_r \ , \tag{6}$$

where p_r is the probability (the relative frequency) that a trajectory is in cell r after N steps. The Kolmogorov entropy characterizes the rate of change in S_N:

$$K_N = \frac{1}{\tau}(S_{N+1} - S_N) \ . \tag{7}$$

The precise definition of K is the average of K_N over the whole attractor (as $N \to \infty$) in the limit of infinite small cells size and time steps ($\tau \to 0$).

One of the most fundamental features of a chaotic system is the divergence of nearby trajectories, which manifests itself as an exponential separation of initially close trajectories as times goes on. This can be interpreted as information loss since the state of a single initial point specified with certain accuracy will not be predictable after evolving for a finite time. The Kolmogorov entropy measures the rate of information loss (or gain) along the attractor. It is usually expressed in bits per second. A positive, finite K is considered as the conclusive proof that the time series and the underlying system are chaotic. K equal to zero represents a regular, cyclic, or constant motion, while an infinite K refers to a stochastic, random phenomenon.

The maximum-likelihood estimation of the Kolmogorov entropy K_{ML} as proposed by Schouten et al.[29] is used in this study, which has the advantage that the uncertainty of the entropy can be easily estimated.

First, the influence of the embedding time window (embedding dimension) on the estimation of K_{ML} is examined. It is proposed[30] that the average cycle time of the oscillations (T_C) provides, in many cases, a robust and characteristic measure for the length of the embedding time window (i.e., $d \cdot T \cdot \tau$). The average cycle time is defined as

$$T_C \equiv \frac{[\text{length of time series (units of time)}]}{[(\text{number of crossings of average of time series})/2]} \ .$$

The value of K_{ML} evaluated for a range of embedding time windows is depicted in Fig. 6. Figure 6 shows that for embedding windows larger than twice the average cycle time, the estimated value of K_{ML} is independent of

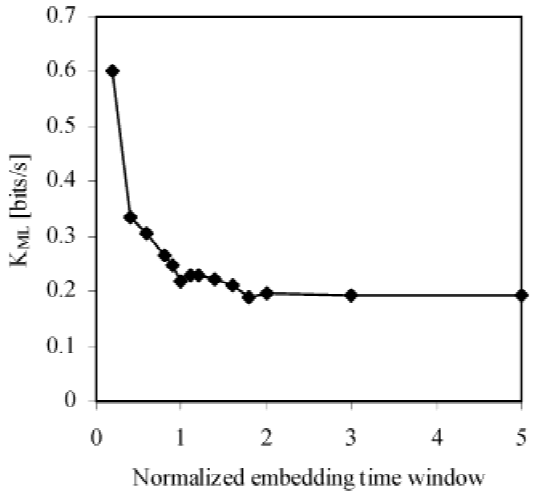

Fig. 6. The influence of the choice of the embedding time window (normalized with T_C) on the estimated Kolmogorov entropy (series 4).

TABLE II

Maximum-Likelihood Estimation of the Kolmogorov Entropy K_{ML}

Series	Power (kW)	Void Fraction K_{ML} (bit/s)	Void Fraction Relative Standard Deviation (%)	Inlet Flow Mass Flow Rate K_{ML} (bit/s)	Inlet Flow Mass Flow Rate Relative Standard Deviation (%)
1	32.3	0.256	0.96	0.211	0.94
2	29.3	0.127	0.93	0.139	0.93
3	31.3	0.044	0.93	0.049	0.91
4	45.9	0.189	0.94	0.116	0.89

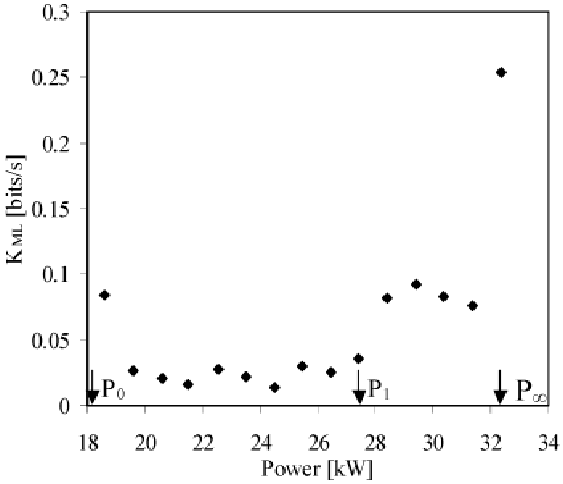

Fig. 7. Evaluation of the Kolmogorov entropy for the different system states (oscillation patterns) as a function of the heating power for series 1. The arrows indicate bifurcation points and the chaotic limit. The Kolmogorov entropy is not zero for the regular oscillation patterns (limit cycle, etc.) due to the influence of noise; however, it remains small and jumps to a significantly higher value once the chaotic limit is exceeded.

the embedding time window. Generally, it is expected that the quantifiers of the reconstructed attractor do not change as a function of the size of the embedding window once the window size necessary to accommodate the attractor is reached.[31] Choosing the embedding window as twice the cycle time, the K_{ML} values evaluated for the different measurements in the four experimental series are summarized in Table II.

It might be interesting (also as a cross-check for the above results) to examine which value of K_{ML} is predicted for the different system states from stable to chaotic, i.e., as a function of the increasing heating power. This is shown in Fig. 7 for experimental series 1. The value of K_{ML} is not exactly zero for the regular oscillation patterns—like limit cycles—as it should be theoretically. This is mainly because of the influence of measurement and inherent noise to which the entropy estimate is sensitive.[29] For example, just after the Hopf-bifurcation point (P_0) where the oscillation amplitude is still quite small, the influence of noise is relatively strong, leading to a high entropy estimate. As the oscillation amplitude increases, the entropy estimate decreases toward zero. It again increases past the first period-doubling point (P_1) because the noise gets relatively stronger again (compared to the small amplitude subharmonics). Finally, K_{ML} jumps suddenly to a distinctly higher value than for the previous states as the power P_∞ is reached, confirming that the system's behavior is indeed chaotic.

III.B.2. The Correlation Dimension

To examine the topological characteristics of the chaotic attractor in state-space, a *geometric* type of chaos quantifier, the correlation dimension, is used. The correlation dimension is proposed by Grassberger and Procaccia[32] based on the behavior of the so-called correlation sum. If one lets the system trajectory evolve for a longer time and collects N trajectory points, then the correlation sum is defined as

$$C(R) = \frac{1}{N(N-1)} \sum_{i=1}^{N} \sum_{j=1, i\neq j}^{N} \Theta(R - |x_i - x_j|) \quad , \quad (8)$$

where Θ is the Heaviside function. If R is about the size of the attractor, then $C(R) \to 1$; if R is smaller than the smallest distance between the trajectory points, then $C(R) = 0$. The correlation dimension D_C is defined to be the number that satisfies

$$C(R) = \lim_{R\to 0} kR^{D_C}$$

or equivalently

$$D_C = \lim_{R\to 0} \frac{\log C(R)}{\log R} \quad , \quad (9)$$

where D_C is also called the scaling index because $C(R)$ scales with it as a function of R. This generalized dimension definition can give dimensionalities that are not integers for fractal objects. Fractals play an important role in the dynamics of chaotic systems since a strange attractor, per definition, has a noninteger dimension.

Generally, measurement noise induces a bias in the observed distances of trajectories and corrupts the scaling behavior expressed in Eq. (9). To calculate D_C, we use the method proposed by Schouten et al.[30] for the case of noisy attractors. This method can disentangle the dimension of the underlying uncorrupted, noise-free

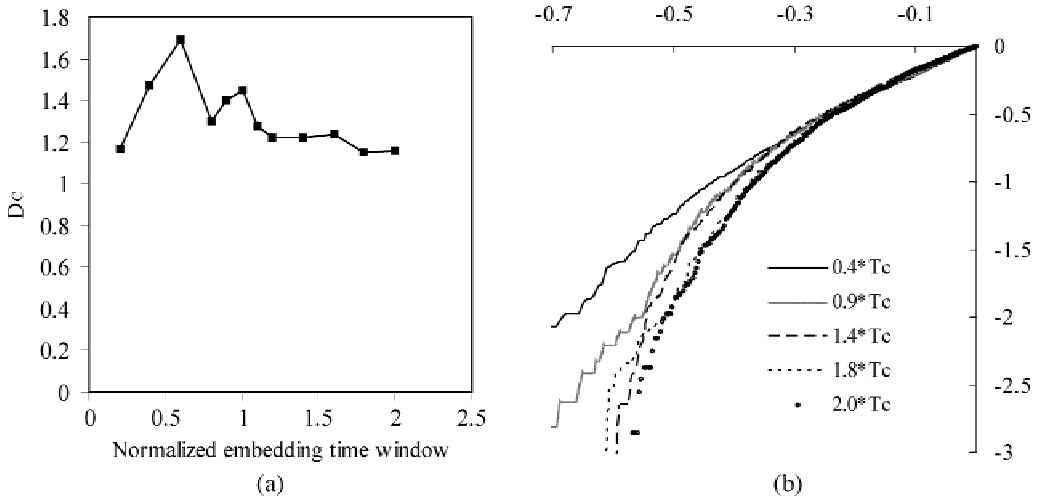

Fig. 8. The behavior of the correlation dimension estimate as a function of the length of the normalized embedding time window (series 4), where (a) shows that similar to the Kolmogorov entropy, the value of the correlation dimension seems to settle as the embedding time window approaches two cycle times and (b) shows the same in terms of the (not-rescaled) $\log C(R)$ versus $\log R$ curves for a sequence of several embedding time windows corresponding to (a). Note that because of normalization, the upper limit of the scaling region is at $\log 1 = 0$, and the lower limit of the scaling region varies around -0.5.

attractor, assuming a bounded-amplitude noise, by rescaling the correlation integral. The method also provides an estimation of the noise level. For the rescaling technique to work fine, the embedding dimension should be chosen to be as large as possible. In practical cases, it is suggested to be at least of the order of 50 (Ref. 30). To be sure about using an appropriate embedding, the behavior of the correlation dimension estimate is also examined as a function of the size of the embedding time window. Figure 8 shows that similar to the Kolmogorov entropy, the value of the correlation dimension seems to settle as the embedding time window approaches two times the average cycle time, which just corresponds to (for our sampling frequency of 4 Hz) an embedding dimension of $\sim$50 as proposed in Ref. 30. Therefore, the correlation dimensions for the four measurement series are evaluated using this embedding window, just as the Kolmogorov entropy, in Table II. The results are presented in Table III. The estimated dimension of the chaotic attractor varies $\sim$1.4 to 1.8 in almost all cases, which indicates a low-dimensional chaotic behavior. The estimated noise levels (r_n) are relatively high, up to 30% of the average absolute deviation of the signals.

Figure 9 shows the behavior of D_C as a function of the increasing heating power. A qualitatively similar trend can be observed as for K_{ML} in Fig. 7, and it can be explained similar to that. For small-amplitude limit cycles, the state-space filling effect of noise leads to a higher dimension estimate. D_C falls to $\sim$1 for large-amplitude limit-cycle and period-two oscillations, with the latter being more sensitive to noise, and finally, it jumps to the value describing the strange attractor for chaotic oscillations.

TABLE III

The Values of the Correlation Dimension and the Noise Level in the Measurement Series*

Series	Power (kW)	Void Fraction		Inlet Flow Mass-Flow Rate	
		D_C	r_n	D_C	r_n
1	32.3	1.738	0.158	1.796	0.206
2	29.3	1.746	0.273	1.831	0.242
3	31.3	1.576	0.287	1.615	0.194
4	45.9	1.203	0.345	1.405	0.301

*r_n is relative to the average absolute deviation of the signal.

III.B.3. The Maximum Lyapunov Exponent

The Lyapunov exponents measure the average exponential rate of divergence or convergence of nearby orbits in state-space and are closely related to the Kolmogorov entropy. Any system containing at least one positive Lyapunov exponent is defined to be chaotic, and the magnitude of the exponent reflects the timescale on which system dynamics become unpredictable. Given a dynamical system in an n-dimensional state-space, one monitors the time evolution of an infinitesimal n-sphere.

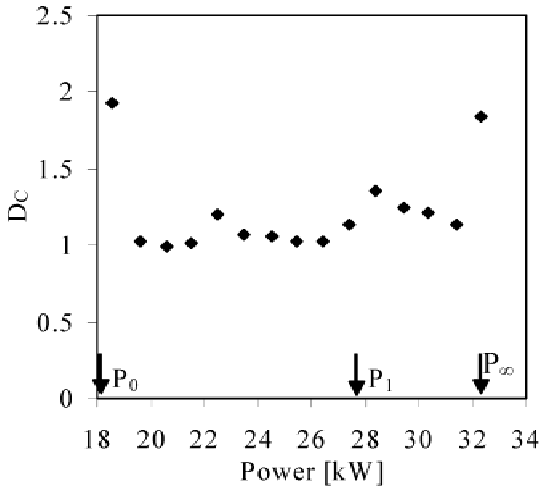

Fig. 9. The behavior of the correlation dimension is plotted as a function of the heating power for series 1. A qualitatively similar behavior is shown as for the Kolmogorov entropy in Fig. 7.

After time t it will be transformed to an n-ellipsoid with principal axes $p_i(t)$, and the i'th Lyapunov exponent is defined in terms of $p_i(t)$ as

$$\lambda_i = \lim_{t\to\infty} \frac{1}{t} \log_2 \frac{p_i(t)}{p(0)} \quad . \tag{10}$$

Thus, the Lyapunov exponents are related to the expanding or contracting nature of different directions in state-space.

The estimation of the largest Lyapunov exponent from the measured time series is based on the method proposed by Wolf et al.[33] The method, which tracks the evolution of two points on nearby orbits of the reconstructed attractor, works as follows: First, the nearest neighbor (in the Euclidean sense) of the first point of the embedded time series is located (we use the same embedding as in Secs. III.B.1 and III.B.2). The distance of the initial points is denoted by $L(t_0)$. At time t_1, this distance increases to $L(t_1)$ as the two points evolve along their trajectories. As the separation between the two points becomes large (comparable to the size of the attractor), the algorithm replaces the second point. In this way one monitors the evolution of a single principal axis vector, and a Lyapunov exponent is estimated for each evolution before each replacement. The replacement attempts to preserve orientation in state-space—so that it keeps following the evolution of the principal axis always in an expanding direction—by trying to minimize the angle between the replacement point and the replaced point. It also minimizes the distance between the evolved first point and the replacement point. The evolution+replacement procedure is repeated until the end of the time series is reached and the set of estimated Lyapunov exponents is averaged to get

$$\lambda_1 = \frac{1}{M} \sum_{k=1}^{M} \frac{1}{t_k - t_{k-1}} \log_2 \frac{L(t_k)}{L(t_{k-1})} \quad , \tag{11}$$

where M is the total number of replacement steps.

In the algorithm proposed by Wolf et al.,[33] the evolution time $t_k - t_{k-1}$ is chosen constant; however, this seems to be a poor estimation of the maximal exponent in our case. Even for an optimized value of the evaluation time, the maximum Lyapunov exponent estimates [Eq. (11)] have high relative standard deviations (200% to 300%). The large scattering in the individual exponent estimates, in addition to the influence of measurement noise, is mainly due to the fixed evolution time. Depending on the position on the attractor, a fixed evolution time can be sometimes so long that one passes from an expanding region to a folding region of the attractor (since for bounded attractors L cannot grow unlimited), which results in an underestimated or even a negative exponent for that evolution and consequently an increased scattering of the mean. On the other hand, choosing the evolution time to be very short would increase the necessary number of replacement steps, which might lead more frequently to momentary loss of following the direction of expansion at replacements. To circumvent these problems, we use variable evolution times: After each replacement we follow the evolution of the distance between the two trajectories until it starts to decrease. At that point, the next replacement step is taken; thus, one always follows the trajectories in the stretching region of the attractor, and the necessary number of replacement steps is decreased as well. To reduce the effect of noise, we reject those evolutions that are shorter than a few time steps (likely due to noise). The maximum Lyapunov exponents estimated with the modified algorithm are summarized in Table IV. Their values vary between 0.23 and 0.36 for the different series, suggesting chaotic system behavior.

TABLE IV

Estimates of the Maximum Lyapunov Exponent Obtained Using a Modified Version of the Method of Wolf et al.*

Series	Power (kW)	Void Fraction		Inlet Flow Mass-Flow Rate	
		λ_1 (bit/s)	Standard Deviation (bit/s)	λ_1 (bit/s)	Standard Deviation (bit/s)
1	32.3	0.23	0.13	0.21	0.12
2	29.3	0.33	0.25	0.30	0.29
3	31.3	0.29	0.19	0.25	0.21
4	45.9	0.36	0.24	0.26	0.18

*Reference 33.

IV. CONCLUSIONS

The nonlinear dynamics of natural-circulation, boiling two-phase flows have been investigated using an experimental two-phase flow loop. Sets of experiments have been carried out in the unstable operating region of the facility for various system pressures and for different frictions at the exit of the riser section. It is found that the two-phase flow undergoes first, a supercritical Hopf bifurcation at the threshold of stability, followed by a period-doubling bifurcation, and finally becomes chaotic as the heating power is increased, which suggests that it undergoes the Feigenbaum scenario. The finer details of the Feigenbaum scenario, i.e., the cascade of period-doubling bifurcations, could not be detected, presumably due to the influence of measurement and inherent noise. To analyze measurements in the chaotic region, nonlinear time sequence analysis methods were applied. Three types of chaos quantifiers have been calculated: the Kolmogorov entropy, the correlation dimension, and the maximum Lyapunov exponent. To find the correct embedding parameters, the influence of the embedding window is examined on the estimated Kolmogorov entropy. It is found that choosing the embedding time window as twice the average cycle time or larger, the attractor is reconstructed correctly. Using these embedding parameters, the estimated values of the Kolmogorov entropy and of the maximum Lyapunov exponent indicate chaotic system behavior. The estimated correlation dimensions suggest low-dimensional dynamics.

REFERENCES

1. J. A. BOURE, A. E. BERGLES, and L. S. TONG, "Review of Two-Phase Flow Instability," *Nucl. Eng. Des.*, **25**, 165 (1973).

2. G. YADIGAROGLU, "Two-Phase Flow Instabilities and Propagation Phenomena," *Thermohydraulics of Two-Phase Systems for Industrial Design and Nuclear Engineering*, p. 353, J. M. DELHAYE, M. GIOT, and M. L. RIETHMULLER, Eds., Hemisphere Publishing Company, New York (1981).

3. R. T. LAHEY, Jr., and F. J. MOODY, *The Thermal-Hydraulics of a Boiling Water Nuclear Reactor*, American Nuclear Society, La Grange Park, Illinois (1993).

4. R. T. LAHEY, Jr., and M. Z. PODOWSKI, "On the Analyses of Instabilities in Two-Phase Flows," *Multiphase Science & Technology*, Vol. 3, Hemisphere Publishing Company, New York (1987).

5. J. L. ACHARD, D. A. DREW, and R. T. LAHEY, "The Analysis of Nonlinear Density-Wave Oscillations in Boiling Channels," *J. Fluid Mech.*, **155**, 213 (1985).

6. RIZWAN-UDDIN and J. J. DORNING, "Nonlinear Stability Analysis of Density-Wave Oscillations in Nonuniformly Heated Channels," *Trans. Am. Nucl. Soc.*, **52**, 404 (1987).

7. RIZWAN-UDDIN and J. J. DORNING, "A Chaotic Attractor in a Periodically Forced Two-Phase Flow System," *Nucl. Eng. Des.*, **100**, 393 (1988).

8. RIZWAN-UDDIN and J. J. DORNING, "Chaotic Dynamics of a Triply-Forced Two-Phase Flow System," *Nucl. Eng. Des.*, **105**, 123 (1990).

9. A. CLAUSSE and R. T. LAHEY, Jr., "The Analysis of Periodic and Strange Attractors During Density-Wave Oscillations in Boiling Flows," *Chaos, Solitons & Fractals*, **1**, 167 (1991).

10. C. J. CHANG and R. T. LAHEY, Jr., "Analysis of Chaotic Instabilities in Boiling Systems," *Nucl. Eng. Des.*, **167**, 307 (1997).

11. P. SAHA, M. ISHII, and N. ZUBER, "An Experimental Investigation of the Thermally Induced Flow Oscillations in Two-Phase Systems," *J. Heat Transfer*, **98**, 616 (1976).

12. M. FURUTERA, "Validity of Homogeneous Flow Model for Instability Analysis," *Nucl. Eng. Des.*, **95**, 65 (1986).

13. D. F. DELMASTRO, A. CLAUSSE, and J. CONVERTI, "The Influence of Gravity on the Stability of Boiling Flows," *Nucl. Eng. Des.*, **121**, 129 (1991).

14. I. S. KYUNG and S. Y. LEE, "Experimental Observation on Flow Characteristics in an Open Two-Phase Natural Circulation Loop," *Nucl. Eng. Des.*, **159**, 163 (1994).

15. I. S. KYUNG and S. Y. LEE, "Periodic Flow Excursion in an Open Two-Phase Natural Circulation Loop," *Nucl. Eng. Des.*, **162**, 233 (1996).

16. R. VAN DER GRAAF, T. H. J. J. VAN DER HAGEN, and R. F. MUDDE, "Scaling Laws and Design Aspects of a Natural-Circulation-Cooled Simulated Boiling Water Reactor Fuel Assembly," *Nucl. Technol.*, **105**, 190 (1994).

17. M. B. PRIESTLEY, *Spectral Analysis and Time Series*, Academic Press, London (1986).

18. R. ZBORAY, A. MANERA, W. J. M. DE KRUIJF, T. H. J. J. VAN DER HAGEN, D. D. B. VAN BRAGT, and H. VAN DAM, "Experiments on Nonlinear Density-Wave Oscillations in the DESIRE Facility," *Proc. 9th Int. Mtg. Nuclear Reactor Thermal-Hydraulics (NURETH-9)*, San Francisco, California, October 3–8, 1999, American Nuclear Society (1999).

19. R. ZBORAY, D. D. B. VAN BRAGT, RIZWAN-UDDIN, T. H. J. J. VAN DER HAGEN, and H. VAN DAM, "Influence of Asymmetrical Axial Power Distributions on Nonlinear BWR Dynamics," *Proc. 9th Int. Mtg. Nuclear Reactor Thermal-Hydraulics (NURETH-9)*, San Francisco, California, October 3–8, 1999, American Nuclear Society (1999).

20. J. HALE and H. KOCAK, *Dynamics and Bifurcations*, Springer-Verlag, New York (1991).

21. M. J. FEIGENBAUM, "The Transition to Aperiodic Behavior in Turbulent Systems," *Commun. Math. Phys.*, **77**, 65 (1980).

22. P. S. LINSAY, "Period Doubling and Chaotic Behavior in a Driven Anharmonic Oscillator," *Phys. Rev. Lett*., **47**, 1349 (1981).

23. M. GIGLIO, S. MUSAZZI, and U. PERINI, "Transition to Chaotic Behavior Via a Reproducible Sequence of Period-Doubling Bifurcations," *Phys. Rev. Lett*., **47**, 243 (1981).

24. H. M. GIBBS, F. A. HOPF, D. L. KAPLAN, and R. L. SHOEMAKER, "Observation of Chaos in Optical Bistability," *Phys. Rev. Lett*., **46**, 474 (1981).

25. C. W. SMITH, M. J. TEJWANI, and D. A. FARRIS, "Bifurcation Universality for First-Sound Subharmonic Generation in Superfluid Helium-4," *Phys. Rev. Lett*., **48**, 492 (1982).

26. J. P. ECKMAN and D. RUELLE, "Ergodic Theory of Chaos and Strange Attractors," *Rev. Mod. Phys*., **57**, 617 (1985).

27. P. GRASSBERGER, T. SCHREIBER, and C. SCHAFFRATH "Nonlinear Time Sequence Analysis," *Int. J. Bif. and Chaos*, **1**, 521 (1991).

28. F. TAKENS, "Detecting Strange Attractors in Turbulence," *Lecture Notes in Mathematics*, Springer-Verlag, Berlin (1981).

29. J. C. SCHOUTEN, F. TAKENS, and C. M. VAN DEN BLEEK, "Maximum-Likelihood Estimation of the Entropy of an Attractor," *Phys. Rev. E*, **49**, 126 (1994).

30. J. C. SCHOUTEN, F. TAKENS, and C. M. VAN DEN BLEEK, "Estimation of the Dimension of a Noisy Attractor," *Phys. Rev. E*, **50**, 1851 (1994).

31. R. C. HILBORN, *Chaos and Nonlinear Dynamics*, Oxford University Press, Oxford (1994).

32. P. GRASSBERGER and I. PROCACCIA, "Characterisation of Strange Attractors," *Phys. Rev. Lett*., **50**, 346 (1983).

33. A. WOLF, J. B. SWIFT, H. L. SWINNEY, and J. A. VASTANO, "Determining Lyapunov Exponents from Time Series," *Physica D*, **16**, 285 (1983).

Robert Zboray (MS, applied physics, Technical University of Budapest, Hungary, 1997; PhD, Delft University of Technology, The Netherlands, 2002) is research engineer at the Laboratory for Thermalhydraulics of the Paul Scherrer Institute, Switzerland. His background includes experimental analysis and modeling of the dynamics of natural-circulation boiling flows and boiling water reactor (BWR) stability.

Wilhelmus J. M. de Kruijf (MS, physics, Eindhoven University of Technology, The Netherlands, 1990; PhD, physics, Delft University of Technology, The Netherlands, 1994) was project manager of BWR research at the Interfaculty Reactor Institute, focusing on BWR stability issues. His background includes reactor physics analyses of the Doppler effect, pressurized water reactor loading pattern optimization, waste transmutation, accelerator driven systems, criticality analyses, and coupled neutronic/thermal-hydraulic transient analysis. Currently he is employed at Erasmus MC Rotterdam as a medical physicist trainee with specialization radiotherapy.

Tim H. J. J. van der Hagen (MS, Eindhoven University of Technology, The Netherlands, 1984; PhD, Delft University of Technology, The Netherlands, 1989) is a full professor in the Department of Applied Sciences of the Delft University of Technology. He heads the Department of Reactor Physics of the Interfaculty Reactor Institute of that university. He has explicit experience in BWR dynamics and specific interest in the interaction between neutronics and thermal hydraulics and in the dynamics of innovative reactor designs.

Rizwan-uddin [BS, mechanical engineering, Middle East Technical University, Ankara, Turkey, 1980; MS, 1983, and PhD, 1987, nuclear engineering, University of Illinois at Urbana-Champaign (UIUC)] is an associate professor in the Department of Nuclear, Plasma, and Radiological Engineering at UIUC. He is also affiliated with the Computational Science and Engineering Program at UIUC. His research interests include reactor operations, BWR stability, two-phase flow dynamics, reactor physics, and computational fluid dynamics.